$C_{exp}$ = experimentally measured concentration, kg·mol/m$^3$
$D_{z,a}D_{z,c}$ = axial dispersion coefficients in the annulus and core, respectively
$D$ = diffusivity of the flowing gas, m$^2$/s
$d_t$ = diameter of the column: $d_c$ = diameter of the core, m
$d_{p,a}, d_{p,c}$ = diameters of the glass beads in the annulus and core, m
$F$ = function to be minimized, Eqs. 20 and 26
$G$ = fractional flow rate, $Q_c/Q$, in the core
$L$ = length of packed column, m
$M$ = strength of pulse input, $\int_o^\infty C^* \, dt$, kg·mol/m$^3$
$\mathrm{Pe}_a$ = Peclet number in the annulus, $V_{z,a}d_{p,a}/D_{z,a}$
$\mathrm{Pe}_c$ = Peclet number in the core, $V_{z,c}d_{p,c}/D_{z,c}$
$Q_a$ = volumetric flow rate in annulus, m$^3$/s; $Q_c$ refers to core and $Q$ represents total flow rate
$[(\mathrm{Re})(\mathrm{Sc})]_a$ = Reynolds number times Schmidt number for the annulus, $V_{z,a}d_{p,a}D/\epsilon_a$
$t$ = time, s; $t_m$ = time corresponding to the maximum concentration in the response curve
$V_z$ = overall superficial velocity, m/s; $V_{z,a}$ and $V_{z,c}$ are superficial velocities in the annulus and core
$Z$ = dimensionless length of packed bed, $z/L$
$z$ = axial dimension in packed column, m

**Greek Letters**

$\delta_a$ = width of the annulus, m
$\delta(\tau)$ = Dirac-delta function, s$^{-1}$
$\epsilon$ = overall void fraction for the entire column; $\epsilon_a$ and $\epsilon_c$ are void fractions in the annulus and core regions
$\mu_1$ = first moment of response curve, s; $\mu_{1,o} = \epsilon L/V_z$, refers to the overall response curve; and $\mu_{1,a}$ and $\mu_{1,c}$ to the annulus and core regions as defined by Eqs. 12 and 13
$\tau$ = dimensionless time, $t/\mu_{1,o}$ or $tV_z/\epsilon L$
$\tau_{m,a}$ = dimensionless time corresponding to the maximum concentration in the response curve for the annulus, $t_{m,a}/\mu_{1,o}$; $\tau_{m,c} = t_{m,c}/\mu_{1,o}$
$\sigma$ = variance of the response curve, s

**Subscripts**

$c$ = core section
$a$ = annulus
$i$ = channel $i$

## LITERATURE CITED


Danckwerts, P. V., "Continuous Flow Systems; Distribution of Residence Times," *Chem. Eng. Sci.*, **2**, 1 (1953).
Ergun, S., "Fluid Flow through Packed Columns," *Chem. Eng. Prog.*, **48**, 89 (1952).
Hsiang, C. T., and H. W. Haynes, Jr, "Axial Dispersion in Small Beds of Large Spherical Particles," *Chem. Eng. Sci.*, **32**, 678 (1977).
Oliveros, G., "Dynamic Experiments for Studying Channeling in Packed Beds," Ph.D. Thesis, Univ. of California, Davis (1981).
Schwartz, C. E., and J. M. Smith, "Flow Distribution in Packed Beds," *Ind. and Eng. Chem.*, **45**, 1209 (1953).
Stanek, V., and V. Eckert, "A Study of Area Porosity Profiles in a Bed of Equal-Diameter Spheres," *Chem. Eng. Sci.*, **34**, 933 (1979).
Wen, C. Y., and Fan, L. T., "Models for Flow Systems and Chemical Reactors," Marcel Dekker Inc., New York (1975).
Wehner, J. F., and Wilhelm, R. H., "Boundary Conditions of Flow Reactor," *Chem. Eng. Sci.*, **6**, 89 (1956).
ZXMIN, "A Computer Program for Minimizing a Function of N Variables," University of California, Davis, Computer Center (1981).



*Manuscript received July 10, 1981; revision received October 29, and accepted November 5, 1981.*


# Heat Transfer to Horizontal Tubes in the Freeboard Region of a Gas Fluidized Bed


**S. E. GEORGE**
**and J. R. GRACE**

**Department of Chemical Engineering**
**and Coal Research Centre**
**University of British Columbia**
**Vancouver, Canada V6T 1W5**



**Overall heat transfer coefficients were measured for an instrumented horizontal tube of diameter 25 mm in the feedboard region above fluidized beds of 102 $\mu$m, 470 $\mu$m and 890 $\mu$m sand in a 0.25 m × 0.43 m × 3.0 m tall pilot scale column. The superficial air velocity varied from near minimum fluidization to 1.7 m/s. The instrumented tube was placed at different positions in a 16-tube bundle. The measured heat transfer coefficients were bounded for tubes near the expanded bed surface by the immersed tube values, and for remote tubes by the values for particle-free air in crossflow. The results are correlated within ±12% by a simple equation which incorporates these limits. The results are in good qualitative and quantitative agreement with previous experimental results.**


## SCOPE

The freeboard region above gas fluidized beds may contain heat transfer tubes for a number of different reasons, e.g., for waste heat recovery, quenching of reaction products, or because of variation in bed level, as in fluid bed combustors during turndown. The tubes are most often horizontal and unfinned. While there have been many studies of heat transfer to tubes immersed inside fluidized beds, tubes in the freeboard region have received scant attention. Experimental results and design methods are required which will allow heat transfer rates to be estimated for tubes in the freeboard region.

In the present study, heat transfer measurements for horizontal unfinned tubes have been carried out in a pilot scale column. Variables have included particle size, superficial air velocity, static bed depth, position within the tube bundle and horizontal pitch. Comparison is given with previous work and with heat transfer for immersed tubes and with tubes subject to crossflow of particle-free air.

S. E. George is presently with the Shell Canada Research Center, Oakville, Canada L6J 5C7.
The experimental work described in this paper was carried out at McGill University, Montreal, Canada.


0001-1541-82-3116-0759-$2.00.

## CONCLUSIONS AND SIGNIFICANCE

**The overall heat transfer coefficients for horizontal tubes in the freeboard region near the expanded bed surface were found to be nearly as favorable as for tubes immersed inside the bed. However, the heat transfer coefficients fell off rapidly with increasing height above the bed surface, approacing the values of particle-free air as the transport disengaging height is approached if the particles are large and heavy enough that entrainment is negligible. The measured heat transfer coefficients were relatively insensitive to position within the tube bundle and horizontal pitch for the ranges of these variables investigated.**

**The experimental results were successfully correlated by means of a simple equation. The experimental results are in qualitative agreement with equipmental results of previous workers. Quantitative comparison is difficult because of differences in flow regime, tube and column geometry, and superficial air velocity. However, our equation is in good agreement with the experimental results of Xavier and Davidson (1981) and Byam et al. (1981) and in fair agreement with those of Wood et al. (1980) in the range where conditions are comparable. The results show a strong influence of particle size, and further work is required with particles outside the size range studied here, as well as for different tube and column sizes and different gas and particle properties.**

### INTRODUCTION

There has been increasing interest in recent years in the freeboard region above gas fluidized beds. This arises not only because no good methods exist for predicting entrainment rates (Matsen, 1979; George and Grace, 1981), but also because chemical reaction rates can be significant in the freeboard (de Lasa and Grace, 1979). In recent years, a number of workers (Aulisio et al., 1975; Howe and Aulisio, 1976; Golan et al., 1979; Wood et al., 1980; Xavier and Davidson, 1981; Tabatabaie-Farashahi et al., 1981; Byam et al., 1981) have also found that heat transfer to tubes in the freeboard region can be quite favorable. This can be important, for example, for coal combustion in fluidized beds, where load-following may be achieved by varying the air flow rate or the solids inventory, hence uncovering tubes, or where additional heat transfer surface may be required to remove sufficient heat, as in pressurized fluidized bed combustion. Tubes may also be used for waste heat recovery or to quench gaseous reception products subject to degradation reactions.

The region immediately above the bed surface is frequently referred to as the "splash zone." Since there is no real way to distinguish the limits of this zone, this term will not be used in the present paper. However, it is useful to distinguish certain types of behaviour near the bed surface. For freely bubbling fluidized beds at relatively low values ($U - U_{mf}$) and large bed diameters, the upper surface is relatively stationary and well defined. Tubes in the freeboard region then encounter particles which are ejected during eruption of bubbles at the surface. If sufficiently small, these particles are carried right out of the column, whereas larger particles decelerate and return to the bed surface under gravity (George and Grace, 1978). At higher values of ($U - U_{mf}$) there is a transition either to the slug flow regime, if the column diameter is sufficiently small and the bed depth sufficiently large, or to the turbulent regime. For the slug flow regime, the bed height rises and collapses in a reasonably periodic manner, and a tube located near the bed surface may be engulfed by the bed intermittently. Many of the results of Xavier and Davidson (1981) were obtained under such slug flow conditions. For the turbulent bed regime, it becomes difficult to distinguish visually the upper bed surface due to chaotic splashing of particles there. Some surging of the surface is also indicated by visual observations. The freeboard heat transfer results reported by Wood et al. (1980) and Ku et al. (1981) were primarily obtained under turbulent regime conditions.

In the present investigation, traces of pressure fluctuations and criteria for entry into the slugging and turbulent regimes indicate that the bed was somewhat too shallow for slugging and the gas velocities too low for turbulent fluidization (George and Grace, 1982). Nevertheless, these transitions are gradual rather than sharp, and some oscillation in dense bed level was apparent.

### EXPERIMENTAL APPARATUS AND PROCEDURE

The experiments were carried out in a stainless steel column of rectangular cross-section ($0.25 \times 0.43$ m) and of overall height 3.0 m. The experimental set-up is described in detail elsewhere (George, 1980; George and Grace, 1981; George and Grace, 1982), so only a brief description is given here. Heat transfer measurements were carried out for a horizontal internally-finned tube of outside diameter 25.4 mm whose surface temperature was measured by eight thermocouples embedded in its surface. Internal cooling was provided by silicone oil whose temperature rise was measured by a differential thermocouple. The freeboard temperature was measured using four chromel-constantan thermocouples and a mercury-in-glass thermometer. The thermocouples were located 30% of the distance from one 0.43 m wall to the other, the position found from transverse temperature profiles to correspond to the mean freeboard temperature (George, 1980). Calculations showed that the gas temperature in the freeboard would differ from the particle temperature by 0.6°C at most, representing a maximum error in the measured heat transfer coefficient of 0.6% for the conditions studied. The bed was heated to a temperature of 385–425 K by means of six inconel electrical heaters braised to the outside surface of the column. At these temperatures, radiation contributed less than 1% of the overall heat transfer coefficient. The results were corrected both for radiation and for conduction from the bed wall through wrapped insulation to the tube.

The instrumented heat transfer tube was located at interior positions in each of the four rows of a 16-tube staggered tube bundle, the other 15 tubes being water-cooled. The lowest row was always located 0.76 m above the distributor. The horizontal centre-to-centre tube spacing could be set at 2.75 $D_T$ or 3.75 $D_T$ while the vertical centre-to-centre pitch was fixed at 3.0 $D_T$. For some experiments, the instrumented tube was on its own. The particles used were silica sand of mean particle size, $\bar{d}_p = -1/\Sigma[w_i/d_{pi}] =$ 102,470 and 890 $\mu$m. Superficial air velocities ranged from $U_{mf}$ (= 0.015, 0.17, and 0.62 m/s for the three sand size fractions) to 1.7 m/s. Mean expanded bed heights were determined from static pressure profiles.

Approximately fifty experimental runs were carried out to investigate the effect of varying superficial air velocity, static bed height, $\bar{d}_p$ and tube configuration. All heat transfer coefficients reported below are time-mean, spacially-averaged outside values. These coefficients were evaluated from the measured temperatures, liquid coolant flow rate and heat capacity and tube dimensions by numerical integration, with conduction along the tube neglected (George and Grace, 1982). Separate experiments were conducted to show that the overall (freeboard-to-oil) resistance was consistent with the sum of the external conduction and internal resistances, and that in-bed and air-alone heat transfer coefficients were consistent with values in the literature (George, 1980; George and Grace, 1982).

### EXPERIMENTAL RESULTS

Figure 1 gives the outside heat transfer coefficient for the instrumented tube in each of the four rows as a function of excess superficial gas velocity for $H_o = 0.75$ m and $\bar{d}_p = 470$ $\mu$m. With increasing air velocity, each of the rows is successively engulfed in the expanded bed. Point C on each curve

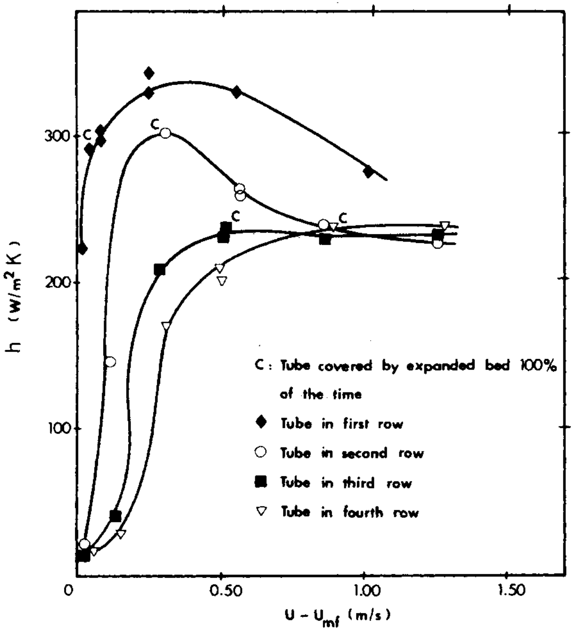


**Figure 1. Heat transfer coefficient for tubes in each row as a function of excess superficial gas velocity for $H_o$ = 0.75 m and $\bar{d}_p$ = 470 $\mu$m.**

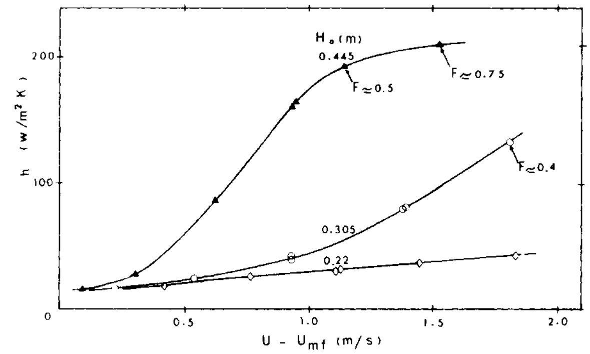


**Figure 2. Heat transfer coefficient for tube in first row, three different static bed depths, and $\bar{d}_p$ = 470 $\mu$m.**

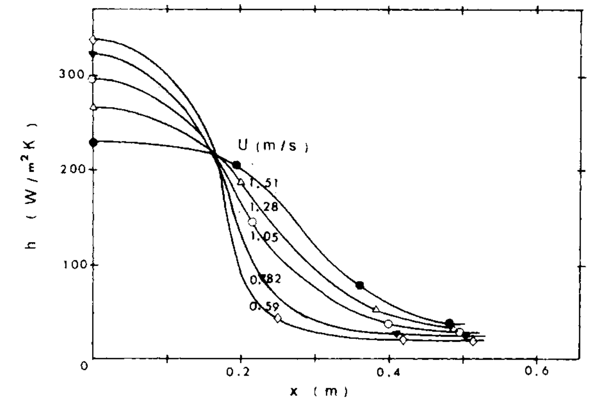


**Figure 3. Variation of heat transfer coefficient with height of tube above expanded bed surface for tube in first row and $\bar{d}_p$ = 470 $\mu$m at different superficial gas velocities.**

gives the air velocity at which the tube is completely immersed in the bed. To the right of point $C$, the coefficients represent bed-to-wall heat transfer for immersed tubes. It is seen that there is a gradual transition towards these in-bed values as the air velocity increases, causing particles to be splashed onto and over the tubes.

Variation of the heat transfer coefficient with excess superficial gas velocity for a tube in the first row is given in Figure 2 for the three static bed heights. The heat transfer coefficient, $h$, for a tube in the freeboard increases

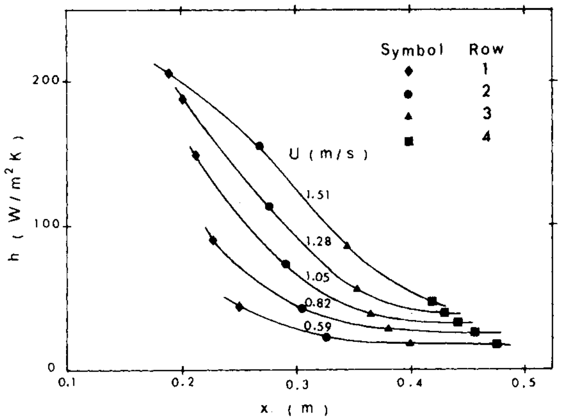


**Figure 4. Variation of heat transfer coefficient within the tube bundle for different superficial gas velocities, $H_o$ = 0.445 m, and $\bar{d}_p$ =- 470 $\mu$m.**

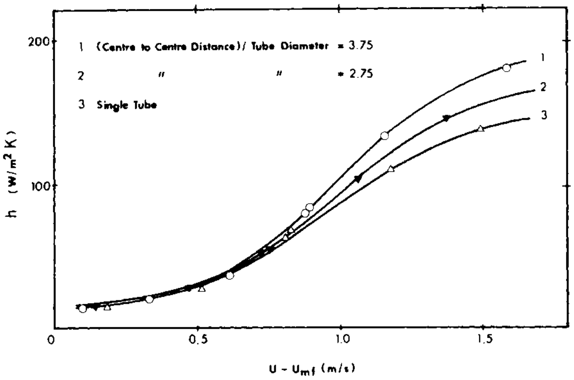


**Figure 5. Effects of tube spacing on heat transfer coefficients for $H$ = 0.445 m and $\bar{d}_p$ = 470 $\mu$m. Curves 2 and 3 are for the tube in the second row of the 16 tube bundles.**

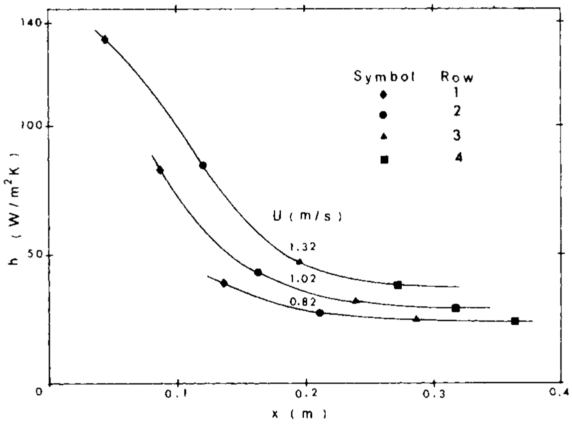


**Figure 6. Variation of heat transfer coefficient within the tube bundle for different superficial gas velocities, $H_o$ = 0.575 m, and $\bar{d}_p$ = 890 $\mu$m.**

with increasing gas velocity as more particles impinge on the tube. For a tube close to the upper surface of the expanded bed, $h$ levels off at higher gas velocities, due to air bubbles engulfing the tube. The fraction of time, $F$, during which the tube was covered by the expanded surface was estimated visually and is shown in Figure 2.

Variation of heat transfer coefficient with height, $x$, measured from the bed surface to the top of tube, is given in Figure 3 for a tube in the first row. The heat transfer coefficient for a tube in the immediate vicinity of the expanded bed ($x < 0.10$ m) is nearly as favourable as in-bed values. Hence, $h$ decreases as $U$ increases near the bed surface for the relatively large values of superficial gas velocity investigated. However, $h$ falls off rapidly with increasing $x$. At higher air velocities, the decrease in $h$ with $x$ is more gradual because of more energetic splashing due to eruptions of larger gas bubbles. This leads to a crossover of the different curves, corresponding to different values of superficial gas velocity. This crossover occurs at $x \simeq 0.17$ m for the conditions pertaining in Figure 3. Variation of transfer coefficients within the bundle itself is shown in Figure 4. It is seen that $h$

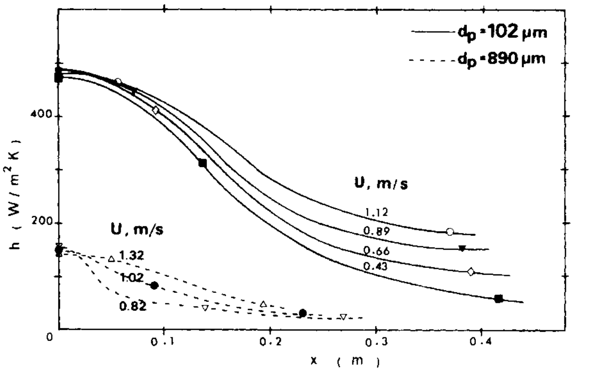


**Figure 7. Variation of heat transfer coefficient with height of tube above expanded bed surface for tube in first row with $\bar{d}_p$ = 102 $\mu$m and $\bar{d}_p$ = 890 $\mu$m.**

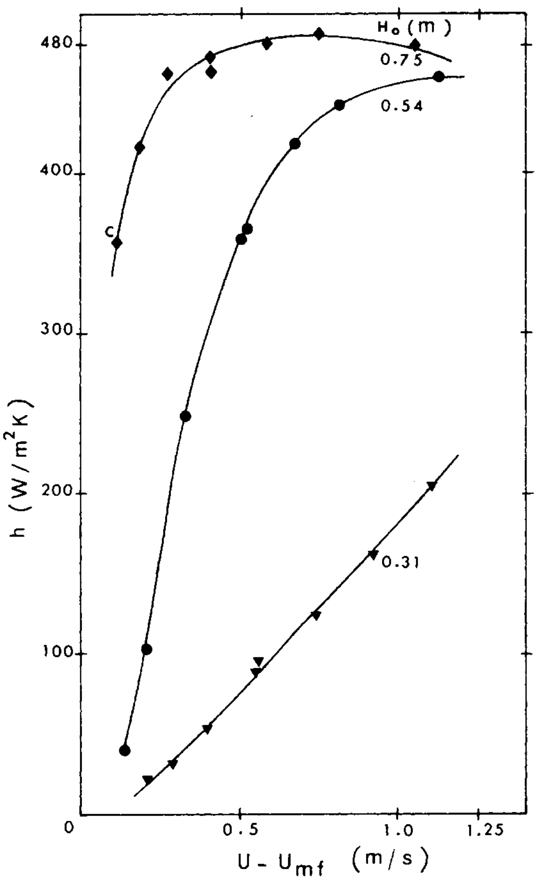


**Figure 8. Heat transfer coefficient for tube in first row, three different static bed heights, and $\bar{d}_p$ = 102 $\mu$m.**

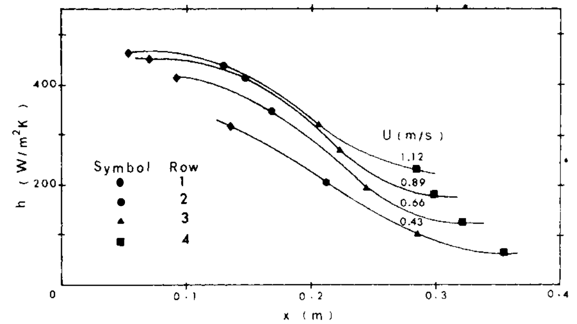


**Figure 9. Variation of heat transfer coefficient within the tube bundle for different superficial gas velocities, $H_o$ = 0.54 m and $\bar{d}_p$ = 102 $\mu$m.**

decreases monotonically from the first to the fourth row for each of the gas flow rates investigated.

Figure 5 shows the effect of horizontal tube pitch on heat transfer coefficients for a tube in the second row and $H_o$ = 0.445 m, again for $\bar{d}_p$ = 470 $\mu$m. Heat transfer coefficients for the more closely packed bundle are somewhat lower than for the more widely spaced bundle. This probably results from increased shielding by surrounding tubes. Transfer coefficients for a single tube were up to 22% lower than that for the wide pitch bundle, possibly due to reduced blockage, and hence lesser air and particle acceleration, leading to decreased particle impingement on the tube.

The variation of transfer coefficient within the bundle for the largest (890 $\mu$m) sand and $H_o$ = 0.575 m is shown in Figure 6. Transfer coefficients fall off rapidly with increasing distance above the expanded bed surface in agreement with results for $\bar{d}_p$ = 470 $\mu$m discussed above. However, $h$ is lower by a factor of up to 3.5.

Variation of $h$ with $x$ for the instrumented tube in the first row is shown in Figure 7 for both the 102 $\mu$m and 890 $\mu$m particles. The trend is similar to that shown by the intermediate particles (compare Figure 3). However, the values of the heat transfer coefficient differ considerably. For the two larger sizes of particles ($\bar{d}_p$ = 470 $\mu$m and 890 $\mu$m) where there is negligible entrainment, $h$ approaches the same limit, $h^o$, the value for particle-free air, with increasing height above the expanded bed surface. For the finest particles, the heat transfer coefficient for the instrumented tube well above the expanded bed surface no longer approaches the limiting values for air alone. This is because of entrainment of fines by the upward-moving air, whereas total disengagement occurred for the larger particles. The $h$ values appear to approach an asymptotic limit, significantly greater than for air alone, corresponding to dilute-phase pneumatically conveyed suspensions. Thie corresponding entrainment rates for this system have been reported for George and Grace (1981).

The increase in the outside heat transfer coefficient with superficial gas velocity is protrayed in Figure 8 for the finest particles. For the deepest bed, $H_o$ = 0.75 m, the instrumented tube was covered over the entire ($U - U_{mf}$) range, and the freeboard heat transfer coefficient for lower static bed heights in seen to approach this limit at sufficiently high gas velocities that the expanded bed surface approached the tube position. The variation of $h$ within the bundle is shown for $H_o$ = 0.54 m and four different superficial air velocities in Figure 9. These results show the same trends as for the two larger sizes of particles (cf. Figures 4 and 6).

## DISCUSSION AND CORRELATION OF DATA

For the two larger sizes of particles where there was negligible entrainment, particles ejected into the freeboard rose, decelerated and fell back onto the bed surface. Very few particles lodged on top of the tubes, and those that did were quickly dislodged. The heat transfer coefficient decreased quickly with increasing height above the bed surface for these cases, approaching the values for particle-free air. The augmentation of the heat transfer coefficient is due to the impingement of particles and disruption of the boundary layer (Andeen, 1974). For the smallest size of particles, there is appreciable carryover into the cyclones (George and Grace, 1981), and the tubes encounter particles even when well above the expanded bed surface. Hence, the heat transfer coefficient no longer approaches the value for particle-free air with increasing height. It was also observed that the smallest particles have a greater tendency to lodge on the tops of the tubes due to splashing.

From the foregoing results and discussion we expect that the heat transfer coefficient will vary monotonically between the in-bed value, $h_b$, close to the dense bed surface to a constant value $h_\infty$ beyond the transport disengaging height. The value of $h_\infty$ will be the air-alone value, $h^o$, correlated by McAdams (1954), when there is negligible entrainment. When there is appreciable carryover, $h_\infty > h^o$. There are no good methods of predicting $h_\infty$ for this case. Glicksman and Decker (1980) have recommended the correlation due to Danziger (1963) as a first approximation. A modified version of the Danziger equation has also been employed by Staub (1979) to predict heat transfer for tubes immersed in turbulent fluidized beds.

In view of these bounds on $h$, it is reasonable to seek a correlation of the form

$$h = h_\infty + (h_b - h_\infty) f(x, U - U_{mf}, \bar{d}_p) \qquad (1)$$

where the function f is expected to vary from 0 to 1 as $x$ increases

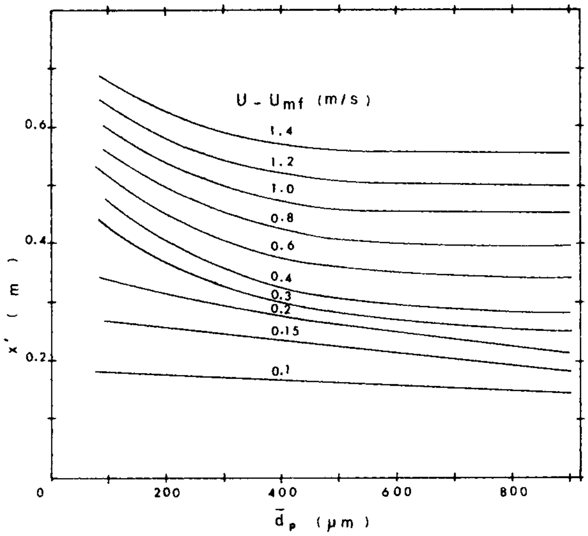


**Figure 10. Height, $x'$, at which $(h - h_\infty)/(h_b - h_\infty)$ reaches a value of 0.025 for conditions in this work.**

from 0 to ∞. It is possible that $f$ will also be a function of certain other variables, e.g., bed diameter, gas properties and other particle properties, but these were not varied in the present study so they have been omitted. Figures 3 and 7 suggest that self-similar profiles are possible if $x$ can be scaled properly. We define a distance $x'$ as the height of the top of the tube, above the expanded bed surface, at which $(h - h_\infty)/(h_b - h_\infty)$ reaches a value of 0.025. This value has been selected to give the best fit with $x/x'$ in the final correlation. A family of $x'$ curves is drawn against $\bar{d}_p$ in Figure 10 for different values of $(U - U_{mf})$ based on our data. For values of $\bar{d}_p$ and $(U - U_{mf})$ not covered by Figure 10, $x'$ appears to be approximately given, for the conditions covered in this work, by

$$x' \simeq TDH/3.5 \tag{2}$$

where TDH is the transport disengaging height predicted by Zenz and Weil (1958).

A functional relationship which satisfies the boundary conditions:

$$(i) \quad h \to h_b \text{ as } X = x/x' \to 0, \text{ and}$$

$$(ii) \quad h \to h_\infty \text{ as } X = x/x' \to \infty$$

is as follows:

$$h = \frac{h_b - h_\infty}{1 + C X^n} + h_\infty \tag{3}$$

where $C$ and $n$ are constants to be determined. Equation 3 also satisfies the additional intuitive constraint that $dh/dx = 0$ at $X = 0$, providing $n > 1$. Rearranging Eq. 3 and taking logarithms, we obtain

$$\log C + n \log X = \log \left(\frac{h_b - h}{h - h_\infty}\right) \tag{4}$$

Figure 11 shows a logarithmic plot of $(h_b - h)/(h - h_\infty)$ vs. $X$ for $\bar{d}_p = 470$ μm. All data points collapse on a straight line independent of $(U - U_{mf})$, although $h_b$, $h_\infty$ and $x'$ are all functions of $(U - U_{mf})$. Similar linear plots were obtained for the other two particle size fractions (George, 1980).

Values of $n$ and $C$ were found using least squares for each $\bar{d}_p$. The values of $C$ turned out to be in the narrow range 33.5 to 34.6 for the three different particle sizes. Hence a single mean value, $C = 34$ has been adopted. With this value of $C$, new fitted values of the index $n$ were obtained by least squares as follows:

(i) For $\bar{d}_p = 102$ μm, $n = 3.4$;

(ii) For $\bar{d}_p = 470$ μm, $n = 5.1$;

(iii) For $\bar{d}_p = 890$ μm, $n = 2.8$.

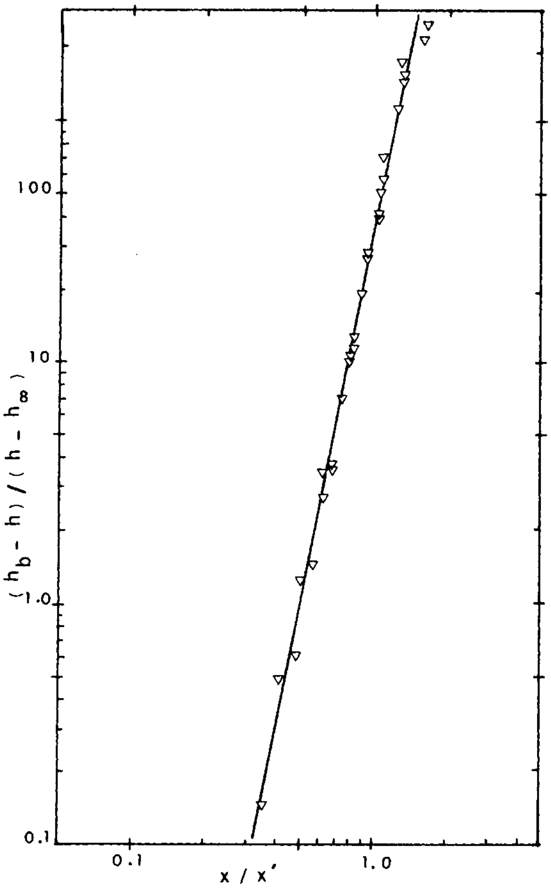


**Figure 11. Data for 470 μm particles fitted according to form of Eq. 4. Line is for $C = 34$ and $n = 5.1$, the fitted values.**

Agreement between our experimental results and Eq. 3 with $C = 34$ and the above values of $n$ is better than ±12%. This is considered to be very favorable considering that bed-to-tube heat transfer correlations for $h_b$ are generally no better than ±50% (George and Grace, 1982). However, $n$ appears to go through a maximum in the range of particle sizes (100–900 μm) investigated in the present work, so that additional work is required for other particle sizes, as well as to show the influence of other factors (e.g., bed diameter, tube diameter, particle properties other than mean diameter, gas properties) not varied in the present study.

Direct comparison of this equation with the results of other workers is rather difficult. For example, the results of Howe and Aulisio (1976) are for an entire tube circuit, with passes at different levels and the range of superficial air velocities, roughly 2 to 5 m/s, did not overlap with that employed herein. Similarly, the high velocity (3 to 10 m/s) turbulent conditions used by Ku et al. (1981) are not directly comparable with the present data. Insufficient detail is given on bed expansion in the paper of Golan et al. to allow a direct comparison. In each of these cases, however, there are qualitative similarities in the data, $h$ dropping from values typical of in-bed conditions to values typical of air alone in cross-flow with increasing tube height above the expanded bed.

Although most of the results of Xavier and Davidson (1981) and Wood et al. (1980) are for the slug flow regime and turbulent regimes respectively, a direct comparison is possible for some of the conditions studied which, by chance, resemble those for the largest particles covered in our own work. In addition, recent measurements obtained by Byam et al. under pressurized (6 bar) fluid bed combustion conditions also lend themselves to direct comparison with our results for the largest sand. The corresponding values are shown in Table 1. While there are differences, especially in column and tube size and geometry, it is clear that conditions were sufficiently similar over a restricted superficial velocity range to allow some comparison to be made.

TABLE 1. CORRESPONDING CONDITIONS IN SEPARATE STUDIES OF FREEBOARD HEAT TRANSFER UNDER COMPARISON

| | Xavier and Davidson (1981) | This Work | Wood et al. (1980) | Byam et al. (1981) |
|---|---|---|---|---|
| Column Cross-Section | 0.305 m square | 0.25 m × 0.43 m | 0.3 m Square | 0.61 m × 0.91 m |
| Particle Type | Sand | Sand | Sand | 20% Coal Ash, 80% Dolomite (Partially Calcined and Sulfated) |
| Mean Particle Diameter | 885 μm | 890 μm | 930 μm | 860 μm |
| Tube Diameter, $D_T$ | 28 mm | 25 mm | 32 mm | 32 mm |
| Horizontal Center-to-Center Tube Spacing | $2.7D_T$ | 2.75 or $3.75D_T$ | $3.2D_T$ | $2.8D_T$ |
| Vertical Center-to-Center Tube Spacing | $2.2D_T$ | $3.0D_T$ | $1.8D_T$ | $2.4D_T$ |
| Fluidizing Gas | Air | Air | Air | Air |
| Temperature | 293 K | 385–425 K | 293 K | 1,030 and 1,160 K |
| Pressure | Atmospheric | Atmospheric | Atmospheric | 6 bar |
| Superficial Velocity | $U_{mf}$ to 1.5 m/s ($U_{mf}$ = 0.45 m/s) | $U_{mf}$ to 1.7 m/s ($U_{mf}$ = 0.62 m/s) | 1 to 5 m/s | 1.2 m/s |
| Bed Height at Minimum Fluidization or Static Bed Height | 0.20 to 0.32 m | 0.22 to 0.75 m | 0.15 to 0.70 m | Not Specified |
| Expanded Bed Height | 0.21 to 0.40 m | 0.23 to 1.0 m | 0.88 to 0.98 m | 1.2 m |

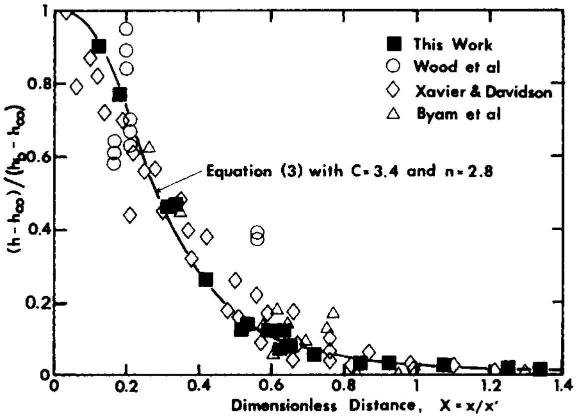


**Figure 12. Comparison between experimental dimensionless heat transfer coefficients and Eq. 3 with $C$ = 34 and $n$ = 2.8. All results are for the bubbling regime and for particles of nearly the same size.**

Results of the studies appear in Figure 12 plotted as a reduced heat transfer coefficient $(h - h_\infty)/(h_b - h_\infty)$ vs. $X$. Equation 3 with $C = 34$ and $n = 2.8$ is also plotted. In plotting the Xavier and Davidson results in this form, $h_\infty$ and $h_b$ are derived from their own data with no particles in the column and the heat transfer surface immersed in the bed respectively. Values of $x'$ were also determined from their own data, and the values turned out to be of order twice the vertical tube pitch and insensitive to superficial gas velocity. This behaviour, which contrasts with our results for $x'$ (Figure 10), probably results from the tighter tube bundle employed by Xavier and Davidson and from the fact that the tube bundle extended right down into the bed so that bubbles erupting at the bed surface would be much smaller than those in the present work where the lowest row of tubes was 700 mm above the distributor. Nevertheless, when $X$ is based on the $x'$ values obtained from the authors' own data, agreement with our correlation is seen to be good.

There were insufficient data to allow $x'$ values to be obtained separately from the Wood et al. study, so values have been obtained from Figure 10. With X derived in this manner, $h_b$ and $h_\infty$ based on data obtained by the authors, and expanded bed heights calculated from the correlations of Staub et al. (1980), the results scatter around the line corresponding to Eq. 3. The point pairs and threesomes at constant $X$ are for adjacent unfinned tubes in the same row and indicate variations in heat transfer horizontally or the degree of reproducibility. Only those results for $U < 2$ m/s are included in the comparison.

In plotting the Byam et al. (1981) results in the form $(h - h_\infty)/(h_b - h_\infty)$ vs. $x/x'$, required by Figure 12, $h/h_b$, $h_\infty/h_b$, $x$ and $x'$ were all obtained directly from the authors' Figure 8. The heights were referred to the height where $h/h_b = 1$. Only the results for the cases where the mean bed height was constant have been plotted here, although the results obtained under conditions where the bed level was gradually rising due to addition of solids do not differ noticeably from those where the inventory of solids was constant. Despite the larger column, the different particle type, the elevated pressure and high temperatures, (high enough that radiative transfer is appreciable), the results of Byam et al. are in good agreement with our own results when plotted in dimensionless form as shown in Figure 12.

The favorable agreement between our correlation and the data in different columns with particles of similar size reported by Wood et al. (1980), Xavier and Davidson (1981) and Byam et al. (1981) suggest that the results are not very sensitive to the factors which did differ between the studies, at least over the range of variation. Differences (Table 1) include the shape and size of the column cross-section, the tube diameter and pitch, the particle density and size distribution, and the air properties (different due to changed pressure and temperature). In view of the complex splashing and eruption patterns at the surface of vigorously bubbling fluidized beds and the wide range of variables which may influence these patterns, the simple correlation procedure presented in this paper should prove to be a useful approach for estimating heat transfer in the freeboard region.

## ACKNOWLEDGMENT

We are grateful to Energy, Mines and Resources Canada and the National Sciences and Engineering Research Council of Canada for financial assistance.

## NOTATION

| | |
|---|---|
| $C$ | = fitted constant in Eq. 3 |
| $D_T$ | = tube diameter |
| $\bar{d}_p$ | = surface-to-volume mean particle diameter |
| $d_{pi}$ | = representative particle diameter for $i^{th}$ size fraction |
| $F$ | = fraction of time tube is immersed in bed |
| $H_o$ | = static bed height |
| $h$ | = heat transfer coefficient |
| $h^o$ | = heat transfer coefficient for gas alone |
| $h_b$ | = heat transfer coefficient for tube immersed in the bed |
| $h_\infty$ | = limiting heat transfer coefficient for tube well above the expanded bed surface |

$n$ = fitted exponent in Eq. 3
$TDH$ = transport disengaging height
$U$ = superficial gas velocity
$U_{mf}$ = superficial gas velocity corresponding to minimum fluidization conditions
$w_i$ = weight of particles in the $i^{\text{th}}$ size fraction
$X$ = dimensionless distance, $x/x'$
$x$ = distance from mean expanded bed surface position to top of tube
$x'$ = value of $x$ at which $(h - h_\infty)/(h_b - h_\infty)$ reaches 0.025

### LITERATURE CITED


Andeen, B. R., "Heat rejection from horizontal tubes to shallow fluidized beds," Ph.D. Dissertation, M.I.T. (1974).

Aulisio, C. J., S. Ehrlich, R. W. Bryers, and J. Bazan, "Fluidized bed performance with internals: heat exchanger above the slumped bed," *Fluidization Technology*, ed., D. L. Keairns, **2**, Hemisphere, 485 (1976).

Byam J., K. K. Pillai, and A. G. Roberts, "Heat transfer to cooling coils in the "splash" zone of a pressurized fluidized bed combustor," *AIChE Symp. Ser.*, **77**, No. 208, 351 (1981).

Danziger, W. J., "Heat transfer to fluidized gas-solids mixtures in vertical transport," *Ind. Eng. Chem. Proc. Des. Dev.*, **2**, 269 (1963).

De Lasa, H. I., and J. R. Grace, "The influence of the freeboard region in a fluidized bed catalytic cracking regenerator," *AIChE J.*, **25**, 984 (1979).

George, S. E., "Heat transfer to tubes in the freeboard region of a fluidized bed," Ph.D. Dissertation, McGill University (1980).

George, S. E., and J. R. Grace, "Entrainment of particles from aggregative fluidized beds," *AIChE Symp. Ser.*, **74**, No. 176, 67 (1978).

George, S. E., and J. R. Grace, "Entrainment of particles from a pilot scale fluidized bed," *Can. J. Chem. Eng.*, **59**, 279 (1981).

George, S. E., and J. R. Grace, "Heat transfer to horizontal tubes in a pilot-scale fluidized bed," *Int. J. Ht. Mass Trans.*, in press (1982).

Glicksman, L. R., and N. A. Decker, "Design relationships for predicting heat transfer to tube bundles in fluidized bed combustors," *Proc. 6th Int. Fluidized Bed Combustion Conf.*, Atlanta, 1152 (1980).

Golan, L. P., D. C. Cherrington, R. Diener, C. E. Scarborough, and S. C. Weiner, "Particle size effects in fluidized bed combustion," *Chem. Eng. Prog.*, **75**, No. 7, 63 (1979).

Howe, W. C., and C. Aulisio, "Trends in heat transfer rates in a fluidized bed steam generator with a submerged horizontal tube circuit," AIChE Annual Meeting, Chicago (Nov., 1976).

Ku, A. C., M. Kuwata, and F. W. Staub, "Heat transfer to horizontal tube banks in a turbulent fluidized bed of large particles," *AIChE Symp. Ser.*, **77**, No. 208, 359 (1981).

Matsen, J. M., "Entrainment research: achievements and opportunities," Proc. N.S.F. Workshop on Fluidization and Fluid-Particle Systems, ed., H. Littman, 452 (1979).

McAdams, W. H., *Heat transmission*, 3rd ed., McGraw Hill, New York (1954).

Staub, F. W., M. Kuwata, A. C. Ku, and R. T. Wood, "Modeling of flow behaviour and finned tube performances in the turbulent flow regime," *Proc. 6th Intern. Fluidized Bec Combustion Conf.*, Atlanta, 784 (1980).

Tabatabaie-Farashahi, M., S. N. Upadhyay, and S. C. Saxena, Fluidized bed and freeboard heat transfer studies with vertical tube bundles, *Letters Ht. Mass Transfer*, **8**, 91 (1981).

Wood, R. T., M. Kuwata, and F. W. Staub, "Heat transfer to horizontal tube banks in the splash zone of a fluidized bed of large particles," *Fluidization*, ed., J. R. Grace and J. M. Matsen, Plenum, New York, 235 (1980).

Xavier, A. M., and J. F. Davidson, "Heat transfer to surfaces immersed in fluidized beds and in the freeboard region," *AIChE Symp. Ser.*, **77**, No. 208, 368 (1981).

Zenz, F. A., and Weil A. N., "A theoretical-empirical approach to mechanism of particle entrainment from fluidized beds," *AIChE J.*, **4**, 472 (1958).



*Manuscript received July 27, 1981; revision received December 8, and accepted January 13, 1982.*


# Numerical Solution of Liquid-Phase Multicomponent Adsorption in Fixed Beds


**A generalized mathematical model is developed to describe the process of multicomponent adsorption on activated carbon in fixed beds. Numerical, finite difference, solutions for the adsorption of binary, and ternary organic mixtures are shown to satisfactorily match previously published experimental data.**



**AWADH MANSOUR,**
**D. U. von ROSENBERG,**
**and N. D. SYLVESTER**

**Department of Chemical Engineering**
**University of Tulsa**
**Tulsa, OK 74104**


## SCOPE

**The removal of pollutants from aqueous waste streams by adsorption onto activated carbon in fixed beds is an important wastewater treatment process. Design and analysis of such systems requires consideration of multicomponent, nonlinear adsorption phenomena in conjunction with intraparticle and interparticle mass transport in a flow system. The objective of this study was to develop a comprehensive mathematical model for multicomponent, liquid phase adsorption in fixed beds and the necessary numerical solution method. Although many investigators have presented models for multicomponent liquid phase adsorption in fixed beds (Tables 1 and 2), the model developed herein is the most comprehensive. It accounts for intraparticle, interparticle and interphase mass transport, non-equilibrium conditions and non-linear multicomponent adsorption. The numerical solution developed permits detailed design and analysis of liquid phase multicomponent adsorption in fixed beds under both steady and unsteady state operation and should be especially useful to pollutant removal from aqueous waste streams.**


Correspondence concerning this paper should be addressed to N. D. Sylvester.
A. Mansour is currently in the Chemical Engineering department at the University of Yarmouk; D. U. von Rosenberg, with Mobile Research in Dallas, TX.


0001-1541-82-6341-0765-$2.00.